Physicochemical Properties of the Novel Heteropolyanion Antiviral Hexapotassium-α-vanado-11-tungstoborate (DuP 925)[1]

Michael B. Maurin,[2,4] Rodney D. Vickery,[2] W. M. Bryant, III,[3] and Munir A. Hussain[2]

Received August 1, 1991; accepted October 31, 1991

Hexapotassium-α-vanado-11-tungstoborate (DuP 925) is a yellow irregular-shaped crystalline powder. The DSC thermogram indicates that decomposition begins to occur above 250°C. The compound exhibits a volatile loss of 3.7% by thermogravimetric analysis. The drug substance adsorbs water reaching a 7.1% volatile loss after 3 weeks at 85% relative humidity. The solubility of DuP 925 in water is high (1.6 g/ml at pH 4.8). Changes in pH have a negligible effect on the solubility with values of 1.3 g/ml in 0.1 *N* HCl and 1.4 g/ml in 0.1 *N* NaOH. The solubility is minimally affected by changes in sodium ion concentration. The compound ion pairs with tetrabutylammonium ions at 1:2 and 1:6 ratios, with the 1:6 ion pair having an affinity over six orders of magnitude greater than that of the 1:2 ion pair. The degradation of DuP 925 in solution follows apparent first-order kinetics over the pH range of 0.6 to 12.6 at 80°C. Citrate, EDTA, and phosphate buffers are catalytic at the pH minimum, with citrate and EDTA being stronger catalysts than phosphate. Acetate buffers appear to have negligible catalytic effects at pH 4 to 5. The degradation proceeds through the formation of the symmetrical dodecatungstoborate $[BW_{12}O_{40}]^{-5}$. In acid, the dodecatungstoborate is stable, while in base it degrades further. Increasing the ionic strength has a catalytic effect on the degradation of DuP 925, while changes in the initial concentration of DuP 925 have a negligible effect on the stability. The pH–rate profile indicates a pH minimum of approximately 3.

KEY WORDS: DuP 925; heteropolyanion; keggin anion; solution stability; ion pair behavior.

INTRODUCTION

Hexapotassium-α-vanado-11-tungstoborate (DuP 925) represents a novel class of compounds known as heteropolyanions (1). It has recently been shown to exhibit antiviral activity by inhibiting reverse transcriptase both *in vitro* and *in vivo* following intravenous administration.

Heteropolyanions are polyoxoion salts of the early transition elements. The heteropolyanions exhibit anomalous behavior in that the overwhelming majority of metal oxides and polyoxoions tends to be insoluble, with poorly understood or limited solution chemistry information available. The formula for heteropolyanions is $[X_xM_mO_y]^{q-}$, with $x \leq m$. In general, M is usually molybdenum or tungsten, or, to a lesser extent, vanadium, niobium, or tantalum, or mixtures of these elements in their highest oxidation states. The metals have the preferred ionic radii and charge and the ability to form $d\pi$–$p\pi$ M–O bonds. The heteroatom X has no restrictions. Keggin determined the structural features of the heteropolyanion lattice (2,3). The X-ray diffraction data demonstrated that the structures were based on MO_6 octahedra as previously suggested (4) but the octahedra were linked with shared edges as well as corners.

For DuP 925, the formula is $K_6[BVW_{11}O_{40}]$, containing 11 tungstates and 1 vanadate. The structural features of DuP 925 have been characterized with one- and two-dimensional ^{183}W and ^{51}V NMR (5).

DuP 925 is a dodecahedral Keggin ion (2) that contains a central boron as the primary heteroatom, surrounded by 12 secondary heteroatoms, that includes 11 tungstates and 1 vanadate with T_d symmetry (Fig. 1). The boron is a BO_4 tetrahedron surrounded by 11 WO_6 and 1 VO_6 octahedra. The 12 octahedra are in four groups of three, having shared edges with three groups of W_3O_{13} and one group of W_2VO_{13}. The four groups of triplets are linked by shared corners to each other and the central BO_4 tetrahedron. It has an overall charge of -6 and is prepared in the form of a hexapotassium salt.

As part of the development of a parenteral dosage form for intravenous administration, the thermal properties, hygroscopicity, solubility, partition behavior, and solution stability of DuP 925 were investigated. The objectives of this study were to determine the thermal behavior and water uptake patterns as a function of controlled humidity, to investigate the solubility profile as a function of pH and the concentration of sodium ions, to provide a thorough understanding of the ion pair interaction, and to evaluate the aqueous stability of DuP 925 as a function of pH, buffer species, ionic strength, initial DuP 925 concentration, and temperature.

MATERIALS AND METHODS

Materials

DuP 925 was prepared by the Chemical Development Section of The Du Pont Merck Pharmaceutical Company, Deepwater, NJ. At the extremes of pH, hydrochloric acid at pH 0.6, 1.2, and 2.2 and sodium hydroxide at pH 11.9 and 12.9 provided sufficient buffer capacity. However, buffers were necessary to maintain the pH in slightly acidic and basic environments. The buffer systems included ethylenediaminetetraacetic acid (EDTA) at pH 2.4, 2.7, and 3.2, citrate at pH 3.0, 4.5, 5.5, and 6, phosphate at pH 3.0, 6.5, and 7.4, acetate at pH 4.0 and 5.0, and borate at pH 9.2. All solvents were HPLC grade. All other reagents were of analytical grade.

Thermal Analysis

The thermal properties of DuP 925 were characterized with differential scanning calorimetry (DSC Model 910, Du Pont instruments) and thermogravimetric analysis (TGA

[1] Presented in part at the fifth annual meeting and exposition of the American Association of Pharmaceutical Scientists in Las Vegas, NV, November 1990.

[2] Pharmacy R&D, The Du Pont Merck Pharmaceutical Company, P.O. Box 80336, Wilmington, Delaware 19880-0336.

[3] Chemical Department, The Du Pont Merck Pharmaceutical Company, Chambers Works, Deepwater, New Jersey 08023.

[4] To whom correspondence should be addressed.

0724-8741/92/0400-0570$06.50/0

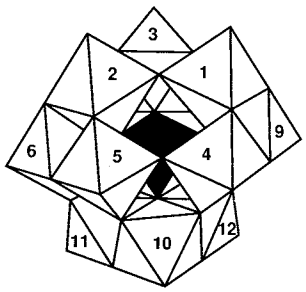

Fig. 1. The Keggin ion structure of $BVW_{11}O_{40}$.

Model 951, Du Pont Instruments), with data analysis via a thermal analyzer (Model 1090, Du Pont Instruments). A heating rate of 10°C/min was employed for both techniques over a temperature range of 25–400 and 25–240°C for differential scanning calorimetry and thermogravimetric analysis, respectively.

Hygroscopicity

The water uptake of DuP 925 was examined with thermogravimetric analysis after incubation at 68, 75, and 85% relative humidities. The humidities were maintained in sealed chambers (Dry Keeper, Samplatec Corporation) with saturated aqueous salt solutions in contact with excess $CuCl_2$, NaCl, and KCl for relative humidities of 68, 75, and 85%, respectively.

Solubility Determination

Solubility studies were carried out by placing excess DuP 925 into a suitable container with the appropriate solvent and rotating end to end for 24 hr at room temperature (22°C). Preliminary experiments indicated that 24 hr provided sufficient time to reach equilibrium. The suspension was passed through a 0.2-μm filter (Acrodisc LC13 PVDF, Gelman Sciences), with the first portion discarded to ensure saturation of the filter. An aliquot of the filtrate was diluted and analyzed by HPLC and the remainder of the filtrate was employed for pH determination.

Partition Coefficient Determination

The partition coefficient of DuP 925 between mutually presaturated octanol and tetrabutylammonium dihydrogen phosphate buffer was followed by measuring the DuP 925 concentration in each phase after shaking (S500, Glas-Col Apparatus Company) for 20 hr at 22°C. The partition behavior was evaluated as a function of tetrabutylammonium ion concentration. Preliminary experiments determined the time to reach equilibrium. Subsequently, 20 hr was employed to ensure complete equilibration.

Solution Kinetics

The DuP 925 was weighed into a suitable container and sufficient buffer was added to result in a 1 mg/ml concentration. The buffer was typically added at room temperature since the samples attained the desired temperature after placement into the stability oven (Model LDX1-42, Despatch Industries, Inc.). For those pH conditions where degradation was rapid, preheated buffer was added to the sample. A constant ionic strength of 0.3 *M* was maintained with the addition of potassium chloride. All solutions were prepared in triplicate. The solution was pipetted into 2-ml glass vials (serum vials 621130-2, Kimble Glass), sealed with Teflon-faced stoppers (4416-50, West Company), and placed in cardboard storage boxes to protect the compound from light. At appropriate intervals, samples were removed from the oven and cooled to room temperature. All buffers were evaluated at three buffer concentrations in order to determine the catalytic effects of the various buffers and to enable extrapolation to zero buffer concentration at any given pH. For those pH conditions where the rate of degradation was rapid, pH 11.9 and 12.9, the sample was immediately quenched to acidic pH by the addition of 0.5 *M* phosphoric acid and cooled to room temperature.

Chromatographic Method

The concentration of DuP 925 was measured with a gradient HPLC method using external standard (6). Separation was performed on a 15-cm reversed-phase Novapak C_{18} column (Waters Chromatography) with the temperature maintained at 40°C (column heater module and temperature control module, Waters Chromatography). The mobile phase was composed of methanol:tetrabutylammonium dihydrogen phosphate, 0.003 *M* (pH 7.3), from 40:60 to 70:30, programmed linearly in 10 min. A flow rate of 1.5 ml/min was employed (automated gradient controller, Model 680, and two HPLC pumps, Model 510, Waters Chromatography). Ultraviolet detection was employed at 210 nm (Spectroflow Model 757, Applied Biosystems). Data acquisition was completed with a VAX-based program that calculated the sample concentrations from a standard curve using peak area with gradient background subtraction (Multichrom software, VG Instruments). The standards were freshly prepared before each analysis.

RESULTS AND DISCUSSION

Thermal Analysis

The DSC thermogram indicated that decomposition of DuP 925 began to occur at temperatures above 250°C. Thermogravimetric analysis revealed a volatile loss of 3.7% that was attributed to water loss. The two steps of weight loss occurred at approximately 105 to 120°C (≈2.5%) and 170 to 180°C (≈1.2%) (Fig. 2). The stoichiometry of the weight loss suggested that the compound is in the form of a hexahydrate.

Hygroscopicity

The compound "as received" had an initial water content of 3.7%. The water content plateaued after 3 weeks at 68, 75, and 85% relative humidities to values of 3.7, 6.2, and 7.3%, respectively. The weight loss profile of samples incubated at 75 and 85% changed from a two-step weight loss to a three-step pattern, with the additional step occurring at approximately 45 to 65°C (Fig. 2), suggesting that the additional 4 to 6 mol of water was adsorbed onto the surface rather than incorporated into the crystal structure.

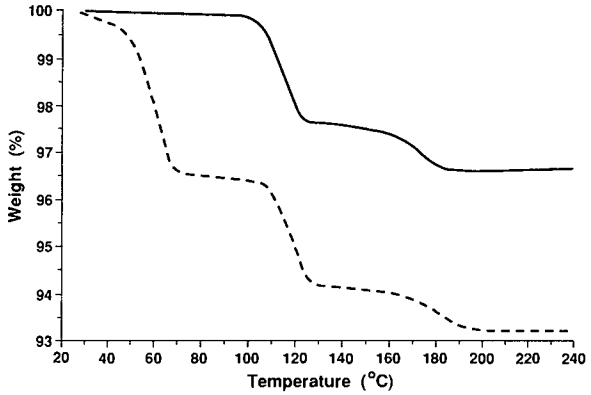

Fig. 2. Thermogravimetric analysis profile of DuP 925 at 10°C/min. DuP 925 exhibited initially a volatile loss of 3.4% in two steps (——), from 105.2 to 122.6°C (2.4%) and from 173.1 to 181.9°C (1.0%). After 3 weeks at 85% relative humidity, the volatile loss of DuP 925 increased to 6.8% in three steps (---), from 47.2 to 67.6°C (3.4%), from 109.3 to 124.9°C (2.4%), and from 182.6 to 190.6°C (1.0%).

Solubility Determinations

DuP 925 dissolved readily into water, forming a brilliant yellow solution. It was very soluble, with an aqueous solubility of 1.62 ± 0.01 g/ml (mean ± SD; n = 3) at pH 4.8. Changes in pH resulted in a negligible effect on its solubility, with values of 1.30 ± 0.03 g/ml (n = 3) in 0.1 N HCl and 1.41 ± 0.04 g/ml (n = 3) in 0.1 N NaOH. The solubility behavior of DuP 925 represented an anomaly compared to most metal oxides in that it was very soluble regardless of pH.

The ability of sodium to displace the potassium either during administration from a normal saline vehicle or after administration by the ubiquitous sodium ions *in vivo* and change the solubility was evaluated by determining the solubility of DuP 925 as a function of sodium chloride concentration at pH 5. Sodium chloride concentrations of 0.15, equivalent to sodium chloride 0.9% (w/v), 0.35, and 0.50 M provided solubilities of 1.43, 1.45, and 1.33 g/ml, respectively. The results indicated that the solubility is minimally effected by changes in sodium ion concentration even when it was in a 200-fold excess relative to the potassium ions, suggesting either that sodium does not displace potassium as the counterion or that the solubility of the sodium salt is equal to or greater than the potassium salt.

Partition Coefficient Determination

The apparent octanol:water partition coefficient of DuP 925 as a function of tetrabutylammonium dihydrogen phosphate concentration at 22°C is presented in Fig. 3. Recovery of DuP 925 from the aqueous buffer and organic phases was greater than 90% based on the initial amount of DuP 925 added for tetrabutylammonium dihydrogen phosphate concentrations of 0.04 M and below. Recovery of DuP 925 was approximately 80% for tetrabutylammonium dihydrogen phosphate concentrations of above 0.04 M. The apparent partition coefficient remained low, less than 0.1, in tetrabutylammonium dihydrogen phosphate concentrations of 0.01 M and below. However, as the tetrabutylammonium dihydrogen phosphate concentration increased from 0.015 to

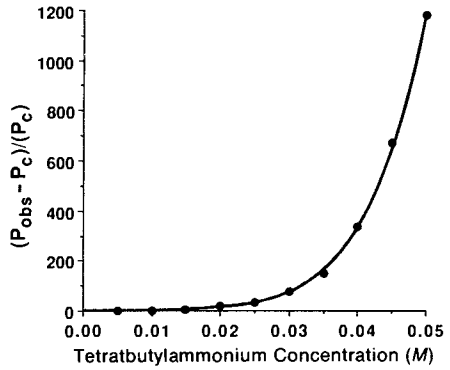

Fig. 3. $(P_{obs} - P_c)/(P_c)$ of DuP 925 as a function of the total tetrabutylammonium dihydrogen phosphate concentration.

0.05 M, the partition coefficient increased exponentially from 0.21 to 33.

The nonlinear partitioning behavior can be attributed to ion pair formation between the heteropolyanion, $[BVW_{11}O_{40}]^{-6}$, and tetrabutylammonium, $(CH_3CH_2CH_2CH_2)_4N+$. The enhanced partitioning behavior may be described by the following relationships:

$$D + nT \rightleftharpoons DT_n \qquad K_{1::n} = \frac{[DT]}{[D][T]^n} \tag{1}$$

where D is the molar concentration of DuP 925, n is an integer, T is the free molar concentration of tetrabutylammonium, DT_n is the molar concentration of the 1:n ion pairs, and $K_{1:n}$ is the 1:n ion pair formation constant. The partition coefficient in the absence and presence of tetrabutylammonium is described below:

$$P_c = \frac{D_o}{D_a} \tag{2}$$

$$P_{obs} = \frac{D_T}{D_a} \tag{3}$$

where P_c is the partition coefficient in the absence of tetrabutylammonium, D_o is the DuP 925 concentration in the octanol phase, D_a is the DuP 925 concentration in the aqueous phase, P_{obs} is the observed partition coefficient in the presence of tetrabutylammonium, and D_T is the total DuP 925 concentration in the octanol phase. D_T is defined by

$$D_T = D + DT_n \tag{4}$$

Combining Eqs. (1) through (4) results in

$$\frac{(P_{obs} - P_c)}{(P_c)} = K_{1:n}[T]^n \tag{5}$$

Since the experiments were carried out with dilute solutions of DuP 925, $T >>> DT_n$; therefore $T \approx T_T$ the total molar concentration of tetrabutylammonium.

$$\frac{(P_{obs} - P_c)}{(P_c)} = K_{1:n}[T_T]^n \tag{6}$$

The polynomial evaluation considered the DuP 925 anion to ion pair with tetrabutylammonium. Polynomials were evaluated for best fit. The optimal correlation coefficient (0.9995)

Table I. Observed First-Order Rate Constants for the Solution Stability of DuP 925 at 80°C

Buffer	k_{obs} (day^{-1})[a]
0.3 *M* HCl, pH 0.6	0.283 ± 4.65×10^{-3}
0.1 *M* HCl, pH 1.2	2.55×10^{-2} ± 5.32×10^{-5}
0.01 *M* HCl, pH 2.2	1.84×10^{-3} ± 3.34×10^{-4}
0.0005 *M* EDTA, pH 2.35	8.18×10^{-2} ± 8.54×10^{-4}
0.001 *M* EDTA, pH 2.35	0.130 ± 5.27×10^{-3}
0.0025 *M* EDTA, pH 2.35	0.210 ± 8.06×10^{-3}
0.001 *M* EDTA, pH 2.7	0.108 ± 2.33×10^{-3}
0.0025 *M* EDTA, pH 2.7	0.130 ± 1.61×10^{-3}
0.004 *M* EDTA, pH 2.7	0.147 ± 1.98×10^{-3}
0.05 *M* phosphate, pH 3.0	1.20×10^{-3} ± 4.79×10^{-4}
0.1 *M* phosphate, pH 3.0	1.32×10^{-3} ± 4.19×10^{-5}
0.2 *M* phosphate, pH 3.0	2.72×10^{-3} ± 3.09×10^{-4}
0.05 *M* citrate, pH 3.0	0.573 ± 3.32×10^{-2}
0.1 *M* citrate, pH 3.0	1.27 ± 2.16×10^{-2}
0.18 *M* citrate, pH 3.0	3.62 ± 0.149
0.25 *M* citrate, pH 3.0	4.24 ± 0.177
0.4 *M* citrate, pH 3.0	6.17 ± 0.636
0.7 *M* citrate, pH 3.0	10.5 ± 0.880
0.01 *M* EDTA, pH 3.2	7.92×10^{-2} ± 3.62×10^{-4}
0.02 *M* EDTA, pH 3.2	0.107 ± 4.28×10^{-3}
0.05 *M* EDTA, pH 3.2	0.151 ± 2.42×10^{-3}
0.05 *M* acetate, pH 4.0	1.73×10^{-4} ± 1.12×10^{-4}
0.1 *M* acetate, pH 4.0	6.79×10^{-4} ± 1.80×10^{-4}
0.25 *M* acetate, pH 4.0	2.67×10^{-4} ± 1.86×10^{-4}
0.05 *M* citrate, pH 4.5	1.29 ± 5.25×10^{-2}
0.1 *M* citrate, pH 4.5	1.77 ± 4.97×10^{-3}
0.18 *M* citrate, pH 4.5	2.20 ± 3.32×10^{-2}
0.05 *M* acetate, pH 5.0	1.86×10^{-3} ± 4.44×10^{-4}
0.1 *M* acetate, pH 5.0	1.61×10^{-3} ± 1.92×10^{-4}
0.25 *M* acetate, pH 5.0	1.74×10^{-3} ± 4.47×10^{-5}
0.02 *M* citrate, pH 5.5	0.555 ± 1.66×10^{-3}
0.05 *M* citrate, pH 5.5	0.629 ± 1.16×10^{-2}
0.1 *M* citrate, pH 5.5	0.790 ± 6.03×10^{-2}
0.013 *M* citrate, pH 6.5	8.22×10^{-2} ± 5.39×10^{-3}
0.03 *M* citrate, pH 6.5	0.146 ± 5.50×10^{-3}
0.065 *M* citrate, pH 6.5	0.286 ± 5.53×10^{-3}
0.05 *M* phosphate, pH 6.5	2.35×10^{-2} ± 1.38×10^{-3}
0.1 *M* phosphate, pH 6.5	2.81×10^{-2} ± 9.67×10^{-4}
0.25 *M* phosphate, pH 6.5	3.20×10^{-2} ± 2.28×10^{-3}
0.05 *M* phosphate, pH 7.4	3.39×10^{-2} ± 1.38×10^{-3}
0.1 *M* phosphate, pH 7.4	5.04×10^{-2} ± 2.26×10^{-3}
0.135 *M* phosphate, pH 7.4	4.19×10^{-2} ± 2.40×10^{-3}
0.05 *M* borate, pH 9.2	1.63 ± 0.104
0.1 *M* borate, pH 9.2	1.92 ± 0.127
0.25 *M* borate, pH 9.2	1.94 ± 4.26×10^{-2}
0.01 *M* NaOH, pH 11.9	24.6 ± 4.08
0.1 *M* NaOH, pH 12.9	185 ± 9.49

[a] Mean ± standard deviation (n = 3).

occurred with the model $y = (2.66 \times 10^4)\,[T]^2 + (7.20 \times 10^{10})\,[T]^6$ (Fig. 3). The apparent lipophilicity of the molecule increased dramatically when the counterion was replaced with a lipophilic substrate, tetrabutylammonium ion. The addition of 0.05 *M* tetrabutylammonium increased the partition coefficient over 3 orders of magnitude, with a preferred ratio of the ion pair of 1:6, which produced a net neutral species due to the −6 of the heteropolyanion and the +1 of the tetrabutylammonium.

Solution Stability

The degradation of DuP 925 followed apparent first-order kinetics. The rate constants were calculated by standard methods with least-squares regression analysis and are listed in Table I. The data from the extremes of pH were employed in the determination of the second-order specific acid and base catalysis rate constants (7). The second-order specific acid and base catalysis rate constants were 0.471 day^{-1} M^{-1} and 32.1 day^{-1} M^{-1}, respectively.

In the intermediate pH range where buffers were employed, the observed first-order rate constant can be defined at any given pH with the following equation:

$$k_{obs} = k' + k_B\,[B_T] \qquad (7)$$

where k' is the observed rate constant extrapolated to zero buffer concentration, k_B is the second-order rate constant for the catalysis due to the buffer, and $[B_T]$ is the total buffer concentration. Plotting k_{obs} vs $[B_T]$ yielded a slope of k_B and a y intercept of k'. The data for the citrate buffers are presented in Fig. 4. The second-order rate constants are provided in Table II. The observed rate constants extrapolated to zero buffer concentration (k') are used to generate the pH–rate profile (Fig. 5). Citrate and EDTA buffers resulted in a tremendous catalytic effect, with the rate of decomposition increased by several order of magnitude. The behavior may be explained by the ability of citrate and EDTA to chelate metals, thereby catalyzing the degradation. Extrapolations to zero buffer concentration from citrate and EDTA buffers produced pH–rate profile behavior that appeared to form an inverted V shape, while the retention behavior of the degradation product remained the same, suggesting that the degradation was dramatically facilitated by the chelating properties of EDTA and citric acid. Acetate and borate buffers did not appear to be catalytic. Where the acetate and borate buffers were employed, k' was determined from the average k_{obs} values for the three buffer concentrations.

The rate constants for the individual buffer species may be calculated utilizing their equilibria expressions. Since the second-order rate constant for the catalysis due to the buffer is the product of the fraction of each buffer species and the second-order rate constant for the catalysis due to the species. Employing the same buffer for various pH conditions permits the determination of the second-order rate constants for the various species (Table III).

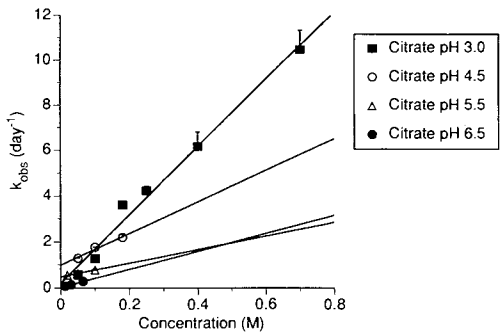

Fig. 4. k_{obs} for the solution stability of DuP 925 vs the total citrate buffer concentration at pH 3, 4.5, 5.5, and 6.5 at 80°C.

Table II. The Second-Order Rate Constants for the Buffer Catalysis and the First-Order Rate Constant Extrapolated to Zero Buffer Concentration for the Solution Stability of DuP 925 at 80°C

Buffer	k' (day^{-1})	k_B ($day^{-1}\ M^{-1}$)
EDTA		
pH 2.35	5.86×10^{-2}	61.6
pH 2.7	9.55×10^{-2}	13.1
pH 3.2	6.66×10^{-2}	1.71
Citrate		
pH 3.0	0.210	14.9
pH 4.5	0.995	6.90
pH 5.5	0.490	2.97
pH 6.5	3.02×10^{-2}	3.92
Phosphate		
pH 3.0	5.02×10^{-4}	1.07×10^{-2}
pH 6.5	2.27×10^{-2}	3.87×10^{-2}
pH 7.4	2.90×10^{-2}	9.49×10^{-2}

The effect of initial DuP 925 concentration on the rate of decomposition was examined in 0.1 *M* phosphate, pH 3.0, at 80°C. Initial concentration of 1, 10, and 32 mg/ml were employed. The results indicate that the degradation of DuP 925 is not concentration dependent at 1 and 10 mg/ml, with rate constants of 5.73×10^{-4} and 5.79×10^{-4} day^{-1}, respectively. At 32 mg/ml, the rate increases two- to threefold, to 1.53×10^{-3} day^{-1}, suggesting that the degradation may be concentration dependent in this range.

The impact of the ionic strength of the buffer system on the rate of decomposition was examined in 0.1 *M* acetate, pH 5.0, at 80°C. Ionic strengths of 0.15, 0.30, and 0.60 *M* were employed. The increases in the ionic strength resulted in an increase in the degradation rate of DuP 925, with the rate constants 3.84×10^{-4}, 6.98×10^{-4}, and 1.20×10^{-3} day^{-1} for ionic strengths of 0.15, 0.30, and 0.60 *M*, respectively. The results suggested that the transition state at pH 5 involves two like charged ions reacting with one another.

The effect of temperature on the reaction rate was evaluated with 0.3 *N* hydrochloric acid and 0.25 *M* borate buffer, pH 9.2. Temperatures of 50, 60, 70, and 80°C were employed. The energy of activation was calculated to be 23.3 and 26.3 kcal/mol for 0.3 *N* hydrochloric acid and 0.25 *M* borate buffer, pH 9.2, respectively.

The retention behavior of the degradation product was evaluated. A single additional peak appeared on the chromatograms. The degradation product had a retention time of 2.5 min, compared to 4.6 min for DuP 925, indicating that the degradation product was more hydrophilic than DuP 925. The most likely cause would be an increase in the net charge from −6 to −5 via the formation of $[BW_{12}O_{40}]^{-5}$. The symmetrical dodecatungstoborate would be expected to be more stable than DuP 925 in acidic solutions. In basic solutions, the dodecatungstoborate forms but it degrades further, probably to Na_2WO_4 and Na_3VO_4. Additionally, an authentic sample of dodecatungstoborate had a retention time identical to that of the DuP 925 degradation samples. A degraded sample of DuP 925 and dodecatungstoborate were mixed together and the mixture produced a single peak on HPLC, providing further evidence for dodecatungstoborate as the degradation product.

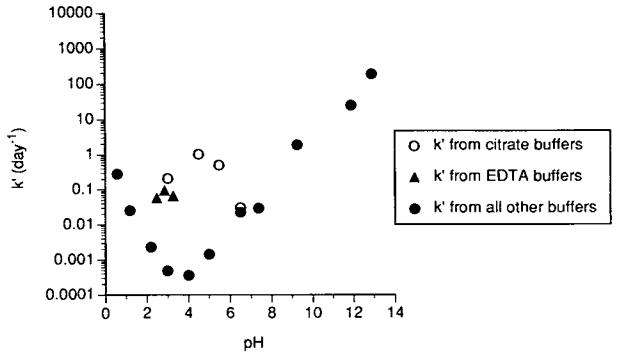

Fig. 5. pH–rate profile for the degradation of DuP 925 at 80°C. All rate values have been extrapolated to zero buffer concentration.

Table III. The Second-Order Rate Constants for the Various Buffer Species for the Solution Stability of DuP 925 at 80°C

Buffer species	k_B ($day^{-1}\ M^{-1}$)
EDTA	242
Citric acid	19.0
Dihydrogen citrate	9.33
Hydrogen citrate	1.30
Citrate	6.03
Dihydrogen phosphate	1.81×10^{-2}
Hydrogen phosphate	0.145

The most likely route involved the formation of a lacunary ion, that is, a Keggin ion devoid of a substituent. The lacunary ion reacted subsequently with a tungstate forming the dodecatungstoborate. The dodecatungstoborate was preferred because of the optimal geometry that resulted from the symmetry of the molecule. The loss of the vanadate was facilitated by its smaller octahedral radii, 0.68 Å, compared to 0.74 Å for the tungstate that would confer an increased ionic mobility (1). The size of the vanadate affected its fit within the W_2VO_{13} triplet and the bonding of the W_2VO_{13} triplet as compared to the W_3O_{13} triplets within the Keggin ion.

ACKNOWLEDGMENT

The valuable discussions with Dr. Y-C. Lee of the Chemical Process group are gratefully acknowledged.

REFERENCES

1. M. T. Pope. *Heteropoly and Isopoly Oxometalates,* Springer-Verlag, New York, 1983.
2. J. F. Keggin. Structure of the molecule of 12-phosphotungstic acid. *Nature* **131**:908–909 (1933).
3. J. F. Keggin. The structure and formula of 12-phosphotungstic acid. *Proc. Roy. Soc. A* **144**:75–100 (1934).
4. L. C. Pauling. The molecular structure of the tungstosilicates and related compounds. *J. Am. Chem Soc.* **51**:2868–2880 (1929).
5. P. J. Domaille. One- and 2-dimensional tungsten-183 and vanadium-51 NMR characterization of isopolymetalates and heteropolymetalates. *J. Am. Chem Soc.* **106**:7677–7687 (1984).
6. Y.-C. Lee. HPLC procedure for E3925 & E3927. Personal communication.
7. H. B. Kostenbauder. Reaction kinetics. In A. Osol (ed.), *Remington's Pharmaceutical Sciences,* 15th ed., Mack, Easton, PA, 1975.